Table 3 Values of α for $w_{max} = qa^4/64D$, $\nu = 0.3$ for a uniformly loaded clamped and simply supported circle

Least squares collocation[6]	Multiple Fourier method				Boundary moments[7]
1.504 (20)	1.499 (42)	1.491 (62)	1.486 (82)	1.481 (122)	1.475 (20)

determining Fourier expansions only for boundary values of r, $1/r$, $\log r$ and finite $1/\rho$ if required, and determining the requisite expansions of Eqs. (4a) and (4b) by raising r and $1/r$ to the appropriate powers and converting the resultant trigonometrical polynomials by addition theorems.

For a uniformly loaded simply supported rectangular plate of dimensions $b \times a$, maximum deflection coefficients are shown in Table 1. The figures in brackets denote the number of nonvanishing terms used in the aforementioned polar series.

A more difficult problem of a uniformly loaded simply supported symmetrical L-shaped plate[4,5] produced the results of Table 2 for deflection across the diagonal between corner points, starting from the outside corner at point 0 and finishing at the re-entrant corner at point 16. Here, a, is the width of the plate with maximum length of $3a$, and d is the proportion of diagonal length traversed. The series above has been truncated at $m = 10$. The results for deflection (and also for moment) are in good agreement with the coupled integral method except near the re-entrant corner. Doubling the number of terms has very little effect on the results, suggesting that within practical limits the correct zero boundary deflection could not be obtained with the series solution adopted. This same problem tackled by a boundary collocation method at this maximum value of $m = 20$ yields very unstable results and far removed from the correct values.

A further problem of a uniformly loaded circular plate clamped and simply supported on alternating quadrants illustrates poor conditioning due to the discontinuity of boundary conditions. Since only $w = 0$ is a common boundary condition a single Fourier analysis cannot be used. Leissa and Clausen[6] solve the problem using least squares point matching and Conway and Farnham[7] use collocation for a boundary distribution of concentrated moments over the clamped segments. Central deflection coefficients for Poisson's ratio, $\nu = 0.3$, are shown in Table 3, the figures in brackets denoting the number of terms used. The convergence of the Multiple Fourier results are slow but uniform and appear to asymptote to the concentrated moment distribution results.

These examples suggest that the method is at least as good as other boundary methods such as least squares and boundary collocation, and when difficulties arise with the type of series solution adopted, slow convergence without instabilities will be indicated. The method is also readily applicable to other boundary value problems with known series solutions within star shaped regions. For example, an elastically supported plate has Bessel function series solutions each of which and its derivatives may be converted into Fourier series in θ.

References

[1] Timoshenko, S. and Woinowsky-Krieger, S., *Theory of Plates and Shells*, McGraw-Hill, New York, 1959.

[2] Robinson, N. I., "Potential Functions and Boundary Collocation in Elastic Plate Analysis," M. E. thesis, 1970, Univ. of Melbourne, Australia.

[3] Pickett, G., "Bending, Buckling and Vibration of Plates with Holes," *Developments in Theoretical and Applied Mechanics*, Vol. 2, 1964, pp. 9–22.

[4] Salvadori, M. G. and Reggini, H. C., "Simply Supported Corner Plate," *Proceedings of the Structural Division, ASCE*, Vol. 86, 1960, pp. 141–154.

[5] Segedin, C. M. and Brickell, D. G. A., "Integral Equation Method for a Corner Plate," *Proceedings of the Structural Division, ASCE*, Vol. 94, 1968, pp. 41–51.

[6] Leissa, A. W. and Clausen, W. E., "Deflection of a Circular Plate Having Mixed Boundary Conditions," *AIAA Journal*, Vol. 5, No. 12, Dec. 1967, pp. 2287–2288.

[7] Conway, H. D. and Farnham, K. A., "Deflections of Uniformly Loaded Circular Plates with Combinations of Clamped, Simply Supported, and Free, Boundary Conditions," *International Journal of Mechanical Sciences*, Vol. 9, 1967, pp. 661–671.

Pressures on Boat-Tailed Afterbodies in Transonic Flow with a Low-Thrust Jet

D. M. Sykes*

The City University, London, England

Introduction

THE pressure over the base of axisymmetric afterbodies varies significantly with Mach number in transonic streams for both cylindrical[1,2] and boat-tailed[3] afterbodies and is known to be influenced by a propulsive jet.[2] Base drag has been reduced by ejecting gas at low flow rates into the base region of a family of boat-tailed afterbodies in both

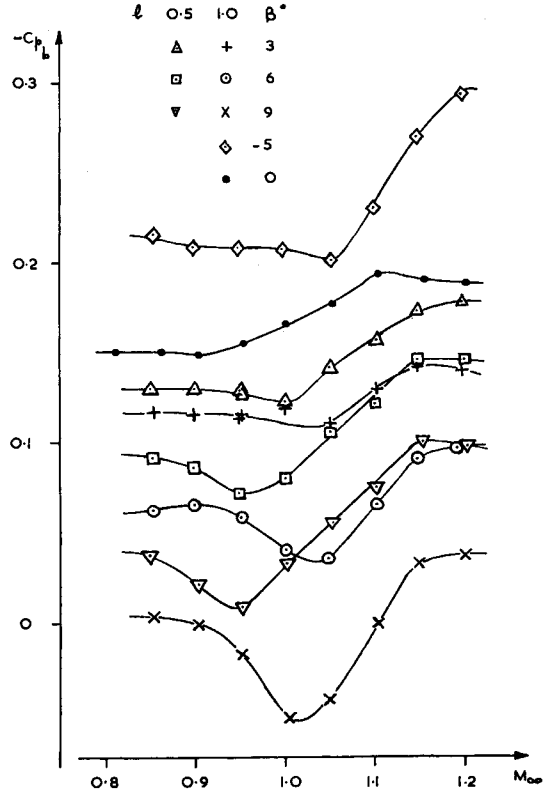

Fig. 1 Base pressure coefficient of various afterbodies.

Received November 5, 1970; revision received January 4, 1971. This work was done while the author was acting as a Vacation Consultant with the British Ministry of Defence. British Crown Copyright reserved. Published with the permission of the Controller of Her Britannic Majesty's Stationery Office.

* Lecturer, Department of Aeronautics.

supersonic[4] and transonic[5] streams. This Note gives further results for pressure distributions on a family of afterbodies at stream Mach numbers from 0.8 to 1.2, and for the effect of a low-thrust jet on these pressures at $M_\infty = 0.95$.

Apparatus

The measurements were made in a continuous running closed return wind tunnel with a 9% open area ratio slotted wall octagonal nozzle of 0.18m inscribed diameter, at Reynolds number increasing with Mach number from 8 to 10 $\times$ 10^6/m. The model, previously used by Bowman and Clayden,[4] consisted of a 50.8-mm-diam hollow centerbody which carried interchangeable 2-caliber long afterbodies. The afterbodies were a straight cylinder, conical boat-tails of $\beta = 3°$, 6° and 9° having length $l = 0.5$ and 1.0 caliber, and a 1 caliber 5° conical flare. Each contained a central nozzle of 10° total cone angle, 0.31D throat and 0.40D exit diameter. Air for the low-thrust jet tests was drawn from the laboratory, metered and fed to the nozzle through the hollow centerbody.

Results

The boundary layer 0.25D ahead of the base of a cylindrical afterbody was investigated at $M_\infty = 0.95$; the velocity distribution conformed to a $\frac{1}{7}$th power law profile with a thickness of 0.09D, which is typical of conventional projectiles.

Pressures measured over the various afterbody bases for $M_\infty = 0.77$ through 1.20 were found to be almost uniform throughout these tests, and the results quoted are average values.

The variation of base pressure coefficient C_{pb} with M_∞ for all the various afterbodies tested is shown in Fig. 1. Increasing β and l both result in an increase of pressure recovered on the base, with maximum C_{pb} being achieved at $M_\infty \simeq 0.95$ for $l = 0.5$ and at $M_\infty \simeq 1.03$ for $l = 1.0$ afterbodies. Crossplots of these data to show variation of C_{pb} with β and l at the various Mach numbers gave nonlinear curves similar to that shown by Sykes[5] for $M_\infty = 0.95$. The distribution of pressure along the surface of the various afterbodies was measured simultaneously with the base pressures and was integrated to give boat-tail drag coefficient $C_{D\beta}$. The variation of $C_{D\beta}$ with M_∞ is shown in Fig. 2 and it can be seen that for $M_\infty < 0.95$ $C_{D\beta}$ increases with β but is almost independent of l, whilst for $M_\infty > 0.95$ increase of β and of l both result in an increase of $C_{D\beta}$, with maximum $C_{D\beta}$ being achieved at $M_\infty \simeq 0.98$ for $l = 0.5$ and at $M_\infty \simeq 1.04$ for $l = 1.0$.

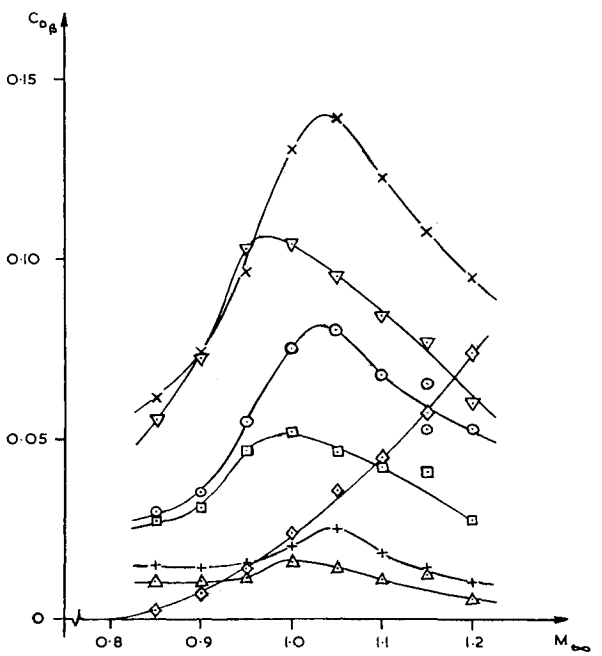

Fig. 2 Boat-tail and flare drag coefficient.

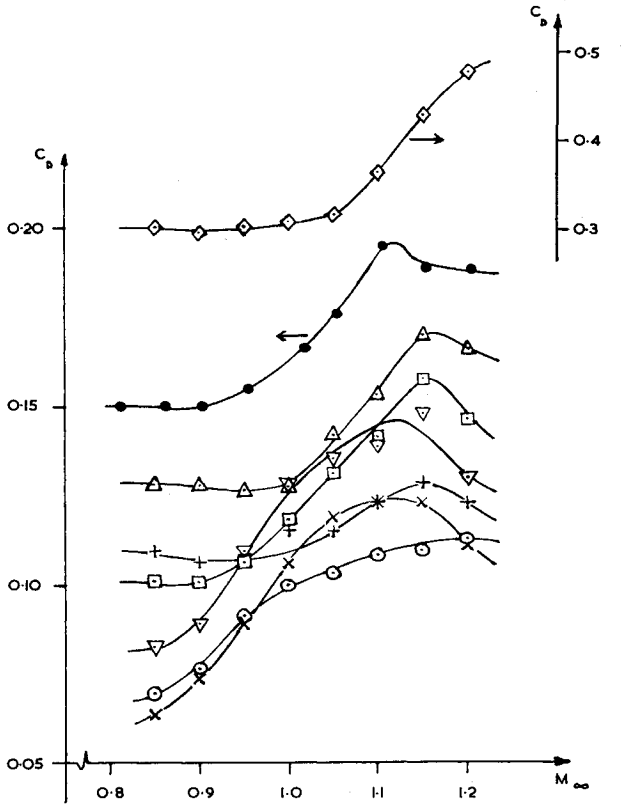

Fig. 3 Afterbody drag coefficient for various geometries.

The afterbody drag coefficient C_D was formed by combining $C_{D\beta}$ and the base area weighted C_{pb} (assumed constant over

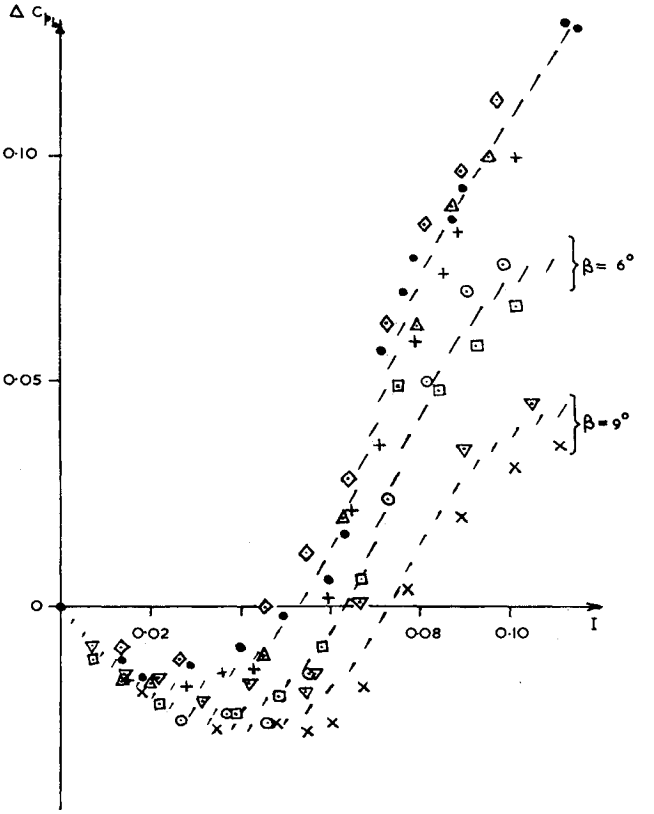

Fig. 4 Base pressure coefficient change with jet flow, $M = 0.95$.

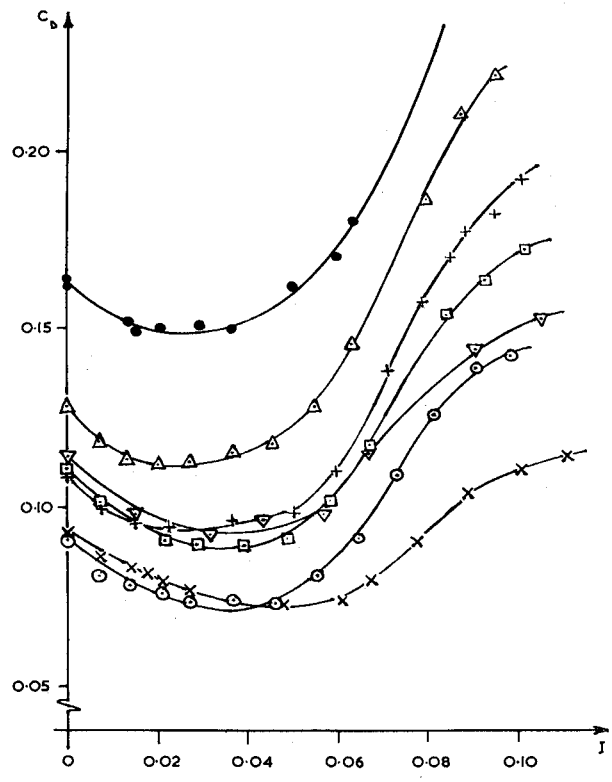

Fig. 5 Afterbody drag coefficient with jet flow, $M = 0.95$.

the nozzle exit) and the variation of C_D with M_∞ is shown in Fig. 3. At the largest values of β the boat-tail drag, which is mainly generated by supersonic expansion around the first shoulder, outweighs the benefit of the increase in recovered base pressure and the afterbody drag is generally higher than that acting on the 6° boat-tail of the same length. A cross-plot of C_D against β for the various Mach numbers showed that the optimum β for minimum afterbody drag through the transonic speed range and with no jet flow is $\beta \simeq 7°$ for $l = 0.5$ and 1.0. This is in agreement with the results of other workers at transonic speeds[3] and at $M_\infty = 2.0$[4].

Pressure distributions over eight afterbodies were measured at $M_\infty = 0.95$ with flow through the nozzle at mass flow rates (relative to stream conditions and centerbody section area) up to $I = 0.11$. The change in base pressure $\Delta C_{pb} = C_{pb}(I = 0) - C_{pb}(I)$ with flow rate I for the various afterbodies is shown in Fig. 4. Initially the base pressures increased with flow rate, but at higher flow rates the base pressure decreased rapidly, as has been indicated previously for cylindrical afterbodies.[2] At low flow rates ($I < 0.03$) Sykes[5] was unable to determine any significant difference in the variation of ΔC_{pb} with I due to differences in afterbody geometry, but the present data indicate that such differences do exist, particularly at the higher flow rates of these tests. It appears from Fig. 4 that, for engineering purposes, the base pressure change on the flare, cylindrical and 3° boat-tail models was almost the same; for $\beta = 6°$ and $\beta = 9°$ the base pressure changes each followed a similar but separate curve with increase of β and l resulting in higher pressure being recovered at slightly higher flow rates in the low flow rate region whilst at the higher flow rates the pressure defects were decreased.

The pressures on the afterbodies near the first shoulder where the flow was locally supersonic were not influenced by nozzle flow rate, but some influence was detected near the base where the flow was locally subsonic. The resulting variation of C_D with I was fairly small, the change being typically about 0.005, and these data were combined with the area-weighted base pressure coefficients (again assumed constant over the nozzle exit) to give afterbody drag coefficients C_D; the variation of C_D with I is shown in Fig. 5. It is immediately apparent from this figure that the adverse effect of higher nozzle flow rate on base pressure is greatly alleviated by boat-tailing, due to the combined beneficial effects of a reduced pressure change from a small pressure defect at zero flow acting on a reduced base area. It is also apparent that whilst at low flow rates the optimum boat-tail angle is about 7°, at higher flow rates the optimum angle is larger.

For cylindrical afterbodies, the variation of C_{pb} with the ratio of jet total pressure to freestream static pressure P_{0j}/P_∞ at $M_\infty = 0.95$ and 1.20 from the present tests has been compared with data of Kurn[2] at $M_\infty = 0.955$ and 1.17 with sonic nozzles having exit to base area ratio $Aj/A = 0.20$ and 0.30. The effect of increasing Aj/A is to increase the base pressure defect at the higher pressure ratios but to reduce the base pressure defect at the lower pressure ratios associated with base bleed conditions.

References

[1] Cubbage, J. M., "Jet Effects on Base and Afterbody Pressures of a Cylindrical Afterbody at Transonic Speeds," RM L56 C21, 1956, NACA.

[2] Kurn, A. G., "A Base Pressure Investigation at Transonic Speeds on an Afterbody containing Four Sonic Nozzles and a Cylindrical Afterbody containing a Central Sonic Nozzle," TN Aero. 2869, 1963, Royal Aircraft Establishment, Farnborough, England.

[3] Silhan, F. V. and Cubbage, J. M., "Drag of Conical and Circular Arc Boat-Tail Afterbodies at Mach Numbers from 0.6 to 1.3," RM L56 K22, 1957, NACA.

[4] Bowman, J. E. and Clayden, W. A., "Boat-tailed Afterbodies at $M = 2$ with Gas Ejection," *AIAA Journal*, Vol. 6, No. 10, Oct. 1968, pp. 2029–2030.

[5] Sykes, D. M., "Cylindrical and Boat-tailed Afterbodies in Transonic Flow with Gas Ejection," *AIAA Journal*, Vol. 8, No. 3, March 1970, pp. 588–590.

Effect of Yaw of Repose on Ballistic Match of Similar Projectiles

H. R. Vaughn* and G. G. Wilson†
Sandia Laboratories, Albuquerque, N. Mex.

Analysis

Yaw of repose results when a gyroscopically stable body is subjected to aerodynamic moments generated by flight path curvature. In a normal shell trajectory, the yaw of repose angle causes the nose of the shell to precess to the right and up from the trajectory for positive spin rates,[1–3] when viewing the shell from the rear (Fig. 1). This causes the shell to drift to the right and above the zero lift trajectory, al-

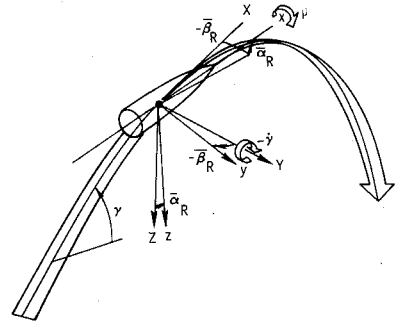

Fig. 1 Yaw of repose.

Received July 9, 1970; revision received February 19, 1971. This work was supported by the U.S. Atomic Energy Commission.

* Supervisor, Aeroballistics Division, Aerothermodynamics Projects Department. Associate Fellow AIAA.

† Member of the Technical Staff, Aeroballistics Division. Member AIAA.